Sci

MDPI

Article

Microplastics in Kidney Stones: A Preliminary Component of an Integrated One Health Investigation

Aniello Primiano [1,*], Lavinia Santucci [1], Michela Cicchinelli [1], Silvia Persichilli [1,2], Paola Roncada [3], Jacopo Gervasoni [1,†] and Andrea Urbani [1,2,†]

[1] Department of Laboratory and Hematological Sciences, Fondazione Policlinico Universitario 'Agostino Gemelli' IRCCS, 00168 Rome, Italy; lavinia.santucci@policlinicogemelli.it (L.S.); michela.cicchinelli@guest.policlinicogemelli.it (M.C.); silvia.persichilli@unicatt.it (S.P.); jacopo.gervasoni@policlinicogemelli.it (J.G.); andrea.urbani@unicatt.it (A.U.)
[2] Dipartimento di Scienze Biotecnologiche di Base Cliniche Intensivologiche e Perioperatorie, Università Cattolica del Sacro Cuore, 00168 Rome, Italy
[3] Department of Health Sciences, University Magna Græcia of Catanzaro, Viale Europa, 88100 Catanzaro, Italy; roncada@unicz.it
* Correspondence: aniello.primiano@policlinicogemelli.it; Tel.: +39-0630158951
† These authors contributed equally to this work.

Abstract

The widespread presence of microplastics (MPs) has emerged as a major One Health concern due to their increasing detection in human tissues and biological fluids. Within an integrated One Health research program, analytical workflows were developed to detect MPs across biological matrices. Kidney stones represent an unexplored pathological biomineral that may preserve evidence of long-term exposure. This pilot study evaluated the application of a Fourier-transform infrared microspectroscopy (μ-FTIR) workflow for detecting MPs in human kidney stones. Sixty kidney stone samples were examined for MPs. Suspected particles identified by stereomicroscopy were chemically characterized by μ-FTIR. Particles were detected in 8 of 60 kidney stone samples. μ-FTIR analysis identified confirmed polyethylene terephthalate (PET), polyethylene (PE), polypropylene (PP), and polyurethane (PU) particles. Additional particles showed absorption bands compatible with polyvinyl chloride (PVC). This study demonstrates the applicability of a μ-FTIR workflow for detecting MPs in pathological biominerals and provides preliminary evidence of their presence in kidney stones. These findings support the use of kidney stones as a novel matrix for One Health biomonitoring and provide a methodological basis for future studies integrating urine, organoids, and multi-omics approaches to investigate the biological significance of microplastic exposure.

Keywords: microplastics; kidney stones; nephrolithiasis; μ-FTIR spectroscopy

Check for updates

Academic Editor: Consolato M. Sergi

Received: 27 July 2026
Revised: 1 September 2026
Accepted: 2 September 2026
Published: 9 September 2026

Copyright: © 2026 by the authors. Licensee MDPI, Basel, Switzerland. This article is an open access article distributed under the terms and conditions of the Creative Commons Attribution (CC BY) license.

1. Introduction

Urolithiasis is one of the most common urological diseases worldwide, and its incidence is steadily increasing [1]. According to the Global Burden of Disease 2021 study, approximately 106 million new cases of urolithiasis occurred worldwide in 2021, with men accounting for approximately two-thirds of cases. Although the absolute number of incident cases increased by 26.7% between 2000 and 2021, the global age-standardised incidence rate decreased by 17.5%, indicating marked heterogeneity in disease trends. The highest age-standardised incidence rates were observed in Eastern Europe, Central Asia,

and Andean Latin America. Recent epidemiological evidence indicates that kidney stone formation results from the interaction of demographic, metabolic, dietary, lifestyle, climatic, and environmental factors [2]. Prevalence has increased in the past decades, with values ranging from 1% to 20% [3]. Environmental factors may contribute to this risk; in particular higher ambient temperatures can increase fluid loss and urinary concentration, thereby favouring stone formation [4]. Recent evidence also suggests a possible association between environmental pollutants and kidney stone disease, particularly exposure to heavy metals such as cadmium and arsenic [5]. These observations support further investigation of emerging environmental contaminants, such as micro- and nanoplastics, and their potential relevance to urinary tract health. The mechanisms underlying kidney stone formation are still not fully understood.

The process of crystal deposition and stone formation is a complex physico-chemical-biological phenomenon. The classical theory of stone formation is based on the concept of urinary supersaturation: when the concentration of lithogenic salts, such as calcium oxalate, calcium phosphate, or uric acid, exceeds the solubility threshold, crystal nucleation occurs, followed by crystal growth and aggregation [6].

Although this model remains fundamental, supersaturation alone does not fully explain lithogenesis, since crystallization may also occur in individuals who do not develop clinically relevant nephrolithiasis. Additional mechanisms, including crystal retention, epithelial interaction, and the presence of anchoring structures, are therefore considered essential for stone development [7].

One of the most important contributions in this field was made by Alexander Randall in the 1940s, when he described the presence of hydroxyapatite deposits at the level of the renal papillae, later termed "Randall's plaques." According to this theory, these plaques act as an initial nidus on which calcium oxalate crystals subsequently deposit, promoting stone growth. The theory of Randall's plaques has since been confirmed by modern endoscopic and histopathological techniques, highlighting the importance of these lesions in stone formation. Alongside the Randall's plaque theory, the hypothesis of "Randall's plugs" has also been proposed. According to this concept, crystals form within the ducts of Bellini under conditions of high urinary supersaturation, obstructing the tubules and creating a favorable substrate for the development of attached stones, which may subsequently detach and grow into clinically significant calculi [8].

Another area of interest concerns the role of high-molecular-weight urinary components, particularly proteins and glycosaminoglycans involved in kidney stone formation. Certain proteins, such as uromodulin (Tamm–Horsfall protein), osteopontin, and other urinary glycoproteins, may act either as inhibitors or, under specific physico-chemical conditions, as promoters of crystallization. In particular, conformational changes or variations in urinary pH may favor their function as a "biological glue," facilitating the mutual adhesion of microcrystals and their stabilization on renal epithelial surfaces. This suggests that the organic matrix of the stone is not merely a secondary byproduct, but rather an active component in the pathogenesis of nephrolithiasis, directly interacting with crystals to promote or inhibit stone formation [9].

Over the last decade, MPs have attracted increasing scientific attention as emerging environmental contaminants with potential implications for human health, animal health, and the environment [10]. Initially investigated mainly as pollutants of marine ecosystems, MPs are now recognized as widespread contaminants across multiple environmental compartments [11]. Their presence in water, sediments, aquatic organisms, food products, air, and drinking water has progressively shifted the field from environmental monitoring to human exposure assessment and biomonitoring [12]. Human exposure may occur mainly through ingestion and inhalation and, to a lesser extent, through dermal contact.

Most larger particles are likely to pass through the gastrointestinal tract and be eliminated in feces, whereas smaller particles, particularly nanoplastics (NPs), may interact with epithelial barriers and reach the circulation. Inhaled particles can also deposit in the respiratory tract and may contribute to systemic exposure. MPs have been detected in human blood [13] and in several tissue suggesting that at least some particles may cross biological barriers and reach internal compartments, although the extent of systemic uptake in humans remains uncertain [14]. The kidney may therefore represent an important site of exposure, and MPs have recently been identified in human kidney tissue [15]. MPs have also been detected in human urine, supporting the possibility of urinary elimination [16]. The presence of MPs in urine does not necessarily demonstrate glomerular filtration, and the mechanisms responsible for their renal handling remain unclear. However, the mechanisms governing their absorption, distribution, persistence, and potential biological effects remain incompletely understood. This uncertainty is particularly relevant for solid biological structures, such as pathological mineral deposits, where exogenous particles may theoretically become entrapped over time.

In this context, a novel hypothesis is emerging regarding the role of MPs present in urine. Recent studies have provided preliminary evidence of MPs in the urinary system and in kidney stones. MPs have been detected in human urine, indicating that some particles can reach the urinary tract, although their biological fate remains uncertain [16]. More recently, MPs were identified in human kidney stones, demonstrating their presence within urinary calculi. However, this finding does not establish whether MPs contribute to stone formation or are incorporated into stones after their formation [17,18]. Experimental studies provide additional evidence for a possible biological effect. In cellular and animal models, polystyrene nanoplastics enhanced renal tubular injury and promoted calcium oxalate crystal deposition [19]. Thus, human studies currently demonstrate the presence of MPs in urine and kidney stones, whereas experimental studies suggest a potential role in stone related renal injury. Whether MPs contribute to the initiation or progression of kidney stones in humans remains to be established.

Although their direct involvement in lithogenesis has not yet been demonstrated, the detection of MPs within kidney stones raises the question of whether these particles may be passively incorporated during stone growth or may actively participate in some phases of the lithogenic process.

Due to their irregular morphology and high surface reactivity, MPs rapidly bind biological macromolecules to form a stable “protein corona” in protein rich biofluids, as demonstrated in gastrointestinal and systemic environments [20,21]. Extrapolating this mechanism to the urological context, MPs excreted or localized in the urinary tract could theoretically undergo similar protein coating, especially under conditions of proteinuria or tubular damage. This microplastic protein complex could subsequently facilitate the adhesion and aggregation of urinary crystals, serving as a nucleation core for crystal deposition within the kidney stone matrix. The physicochemical properties of MPs may also contribute to their interaction with urinary crystals. However, the presence of MPs within kidney stones does not demonstrate that they act as nucleation sites, and this possibility remains to be confirmed experimentally.

Although still speculative, this hypothesis opens new perspectives for research into the possible link between environmental pollution and the increasing incidence of urological diseases.

In the present pilot biomonitoring study, we analyzed kidney stone samples obtained from patients undergoing surgical treatment or from individuals who spontaneously expelled renal calculi.

Using stereomicroscopic examination followed by micro-Fourier transform infrared spectroscopy (μ-FTIR), we investigated the presence, morphology, localization, and polymeric composition of suspected microplastic particles embedded within kidney stones. This study aimed to provide preliminary evidence on the incorporation of MPs into urinary calculi and to support future investigations on their potential role in stone formation.

2. Materials and Methods

2.1. Chemicals

Water was purchased from Biosolve (Biosolve Chimie, Dieuze, France). Ethanol was purchased from Carlo Erba (Carlo Erba Reagents srl, Milan, Italy). All reagents were of analytical grade or higher. Silver membrane filters were purchased from Sterlitech (Sterlitech Corporation, Auburn, WA, USA). Gold-Coated Microscope Slides were purchased from Platypus Technologies (Madison, WI, USA). Cellulose nitrate filters were purchased from Sartorius (Sartorius AG, Gottinga, Germany).

2.2. Kidney Stones Collection

In our laboratory, routine kidney stone analysis includes a morpho-constitutional evaluation, as previously described in our 2018 study [22]. During the initial phase of the morphological assessment, particular attention was paid to the identification of possible non-crystalline particles within the calculi for further characterization. Over the past five months, this approach was applied to 60 kidney stone samples submitted for routine analysis, obtained either from patients undergoing extracorporeal lithotripsy or from individuals who had spontaneously expelled renal calculi. Each sample was morphologically examined using a stereomicroscope. In the case of stones obtained after extracorporeal shock wave lithotripsy, all available fragments were examined. In the case of intact stones, the external surface was first inspected, and the stone was subsequently sectioned to expose the internal regions, including the nucleus and intermediate layers.

To minimize the risk of contamination, kidney stones were rinsed with pre-filtered water before analysis. Particles located on the external surface of the stones were not considered for μ-FTIR characterization. This distinction between surface particles and particles embedded within the internal regions of the stone was considered essential to reduce the risk of false-positive identification due to environmental or handling-related contamination. Surface particles were excluded because they were considered more likely to derive from collection, transport, or laboratory manipulation. Conversely, particles entrapped within the nucleus or intermediate layers of the stone were considered more informative for evaluating possible incorporation during stone growth; therefore, only particles firmly embedded within the crystalline structure and identified after stone sectioning or fragmentation, specifically in the nucleus or intermediate layers of the calculus, were selected for further analysis.

The portion containing the suspected microplastic particle was transferred into a glass container using metal forceps. All procedures were performed under a laminar flow hood, and the samples were stored at −80 °C until analysis. Subsequently, the remaining portions of the calculi were analyzed by attenuated total reflectance (ATR) spectroscopy (PerkinElmer, Shelton, CT, USA) to determine their biochemical composition. The study protocol was approved by the Ethics Committee and conducted in accordance with the Declaration of Helsinki.

2.3. Quality Assurance and Quality Control

Throughout all procedures, including sample collection, storage, and analysis, preventive measures were adopted to minimize the risk of exogenous microplastic contamination.

Operators wore cotton laboratory clothing and latex gloves. Sample handling and storage procedures were carried out under a laminar flow hood dedicated exclusively to this specific analysis. All glassware, reflective slides and metal instruments were thoroughly cleaned with 70% ethanol and pre-filtered water before use and dried in an oven.

Procedural blanks were included in each analytical session. Specifically, whenever a reflective slide was used for sample analysis, an additional clean reflective slide was used as a procedural blank and left exposed under the laminar flow hood (Arredi Tecnici Villa S.p.A., Caronno Pertusella, VA, Italy) throughout the entire experimental procedure. At the end of the analytical session, the blank slide was inspected using both a stereomicroscope and the optical microscope coupled to the infrared spectrometer in order to verify the absence of contaminating MPs from the working environment.

To minimize contamination, kidney stones were rinsed with filtered water upon arrival and subsequently stored in Pyrex glass containers (SciLabware Limited, Stoke-on-Trent, Staffordshire, UK). Although samples were initially transported in polystyrene falcon tubes, no polystyrene particles were identified among the detected MPs. To evaluate potential contamination from the tubes, three falcon tubes filled with filtered water were maintained for 1 h at room temperature, corresponding to the maximum sample handling time. μ-FTIR analysis of the filtered water revealed no polystyrene particles, indicating that sample transport in falcon tubes did not contribute detectable contamination.

2.4. Identification and Characterization of MPs

2.4.1. Analysis by Stereomicroscope

The kidney stone samples were analyzed using a stereomicroscope (SMZ 168—Motic, Cabrera de Mar, Barcelona, Spain) and observed at different magnifications (from 7.5× up to 50×). In the case of kidney stones obtained after extracorporeal shock wave lithotripsy (ESWL), all available fragments were studied while for intact stones after surface observation the kidney stone was dissected and the internal parts were visualized in the search for MPs. Visual inspection of the kidney stone samples was conducted under a stereomicroscope within a laminar flow hood to prevent external contamination. During stereomicroscopic examination, suspected particles were evaluated according to their morphology, color, relationship with the surrounding crystalline material, and degree of adhesion or entrapment within the stone matrix. Particles located on the external surface, without evidence of incorporation into the stone matrix, were excluded from further analysis. When a suspected particle was identified within an internal region of the calculus, the corresponding stone fragment was isolated using stainless steel forceps and transferred for spectroscopic characterization. The investigated particles were classified in according to their shape and color.

2.4.2. Analysis by μ-FTIR

Subsequently, the collected MPs were identified using a PerkinElmer Spectrum Two FTIR spectrometer equipped with a Spotlight 200i microscope (PerkinElmer, Shelton, CT, USA). The detector type was liquid nitrogen-cooled mercury cadmium telluride, all particles were analyzed with a magnification of 10×, and the spectral region investigated was from 4000 to 600 cm^{-1} at resolution 4 cm^{-1}. Particles that adhered well to the slide were analyzed by micro-attenuated total reflectance Fourier-transform infrared (μ-ATR-FTIR) spectroscopy (PerkinElmer, Shelton, CT, USA), whereas particles that did not allow sufficient contact with the ATR crystal were deposited onto reflective substrates, such as gold coated slides or silver membrane filters, and analyzed in Fourier-transform infrared microspectroscopy in reflectance mode (μ-FTIR reflectance). A background spectrum was collected before every analysis: for μ-ATR-FTIR analysis, background spectra were collected

in air, while for μ-FTIR reflectance mode, background spectra were acquired using a gold or silver mirror.

After spectrum acquisition using the functions available in the Perkin Elmer Spectrum software (version 10.6.2), baseline correction was performed using the same software to obtain spectra suitable for spectral matching. Subsequent spectral preprocessing was performed directly through the OpenSpecy web interface before spectral comparison. Prior to library matching, spectra were preprocessed using the built-in functions Conform Wavenumbers, Min–Max Normalize, and Smoothing/Derivative, using the default settings provided by OpenSpecy.

Spectra were recorded by means of a Perkin Elmer Spectrum version 10.6.2.

Following μ-FTIR data acquisition, spectral interpretation was performed through a three-step workflow. First, the spectra were visually examined to identify the main diagnostic absorption bands, which were assigned by comparison with characteristic bands reported in the literature. Second, spectral identification was supported using the OpenSpecy web interface [23,24]. Prior to library matching, spectra were preprocessed using the built-in Conform Wavenumbers; Min–Max Normalize and Smoothing/Derivative functions. The processed spectra were then compared with the OpenSpecy reference spectral library, and the best match value and the corresponding material class were recorded. Finally, the results obtained from the automated library search were critically evaluated against the visual interpretation of the spectra and the literature data. Therefore, OpenSpecy 1.0 was used as a complementary tool to support material identification rather than as the sole basis for spectral assignment. Polymer assignments were considered confirmed when the diagnostic μ-FTIR absorption bands were consistent with the expected polymer and OpenSpecy matching supported the same material class. An acceptable match was assigned when visual inspection of the spectrum showed at least three characteristic absorption bands and a spectral library match value >0.7. A good match was assigned when at least three characteristic absorption bands were present and the spectral library match value was >0.8. Spectrum samples exhibiting at least three characteristic bands of a given polymer, but for which spectral library matching did not yield a corresponding result, were classified as putative and interpreted with caution.

This criterion was particularly relevant for particles analyzed in μ-FTIR reflectance mode, because the OpenSpecy database is largely based on reference spectra acquired in μ-ATR-FTIR mode, which may reduce the accuracy of automated library matching when applied to reflectance spectra.

2.5. Biochemical Composition of Kidney Stones

The spectroscopic analysis was performed by Spectrum two-Perkin Elmer Spectrometer (Perkin Elmer, Shelton, CT, USA) with an attenuated total reflectance (ATR) accessory(Perkin Elmer, Shelton, CT, USA). The stones were powdered and put onto the diamond crystal of the ATR accessory. The spectrum was recorded in the wave number range of 4.000–400 cm^{-1} with a 4 cm^{-1} resolution. The ATR crystal was cleaned with distilled water and ethanol before every acquisition. The acquired spectra were subsequently compared using the spectral library search function of the Spectrum software (kidney stone spectral library), which matches the unknown spectrum against reference spectra contained in the library over the range of 4000–400 cm^{-1}. A report was then generated identifying the different stone components and their relative spectral matches.

3. Results

MPs were identified in 8 of 60 kidney stone samples including confirmed polyethylene terephthalate (PET), polyethylene (PE), polypropylene (PP), and polyurethane (PU)

particles. Three additional particles showed spectral features compatible with polyvinyl chloride (PVC), for this reason classified as putative (p-PVC). Considering only confirmed polymer identifications, MPs were detected in 5 of 60 samples (8.3%; 95% CI: 2.76–15.89%). When p-PVC particles were included, the overall prevalence was 8 of 60 samples (13.3%; 95% CI: 5.94–24.59%). This positivity rate should not be interpreted as an estimate of the prevalence of MPs in kidney stones, since only particles visually suspected to be MPs were selected for μ-FTIR confirmation.

The biochemical composition of the kidney stones is reported in Table 1. No particles compatible with MPs were observed in procedural blanks during stereomicroscopic or μ-FTIR inspection.

Table 1. Biochemical composition of the analyzed kidney stones determined by FTIR spectroscopy and number of particles detected in each stone. COM: calcium oxalate monohydrate; COD: calcium oxalate dihydrate; CA: carbonate apatite; PAM: magnesium ammonium phosphate; AU0: anhydrous uric acid; AU2: dihydrate uric acid; AmUr: ammonium urate; PR: proteins; Br: Brushite.

Substances Detected	Nr.	KS with Particles	(%)
COM	16	1	12.5
CA + COM + PR	3	2	25.0
CA + PAM	3	0	0
CA + PAM + COM	1	0	0
AU0 + AU2	1	0	0
AU0 + COM	4	0	0
Br	1	1	12.5
COM + CA	8	0	0
COM + COD + CA	14	3	37.5
COM + COD	5	1	12.5
AU0	2	0	0
CA + PAM + COM + AmUr	1	0	0
CA + PAM + AmUr	1	0	0
tot	60	8	100

Eight particles were detected in eight kidney stone samples and categorized according to abundance, size, color, localization within the stone, and chemical characterization. Fiber width, estimated from the calibrated scale of the Spotlight 200 micro-FTIR imaging system, ranged from 8 to 17 μm. For some fibers, the exact length could not be reliably determined, and therefore compliance with the adopted microplastic size definition could not always be confirmed (fiber length could not be reliably determined because the fibers were frequently folded and curved and, being entrapped within the crystalline matrix, could not always be completely extracted without risking fragmentation or loss of material). Morphoconstitutional analysis showed that two particles were located within the stone nucleus, one particle was identified spanning both the nucleus and the intermediate region, and four particles were found exclusively within the intermediate region. In one additional disintegrated specimen, the original stone architecture was not preserved, and particle localization could not be reliably assessed.

The identified particles exhibited a range of colors, including dark blue, light blue, white and red. A comprehensive summary of particle features is provided in Table 2.

All detected MPs were analyzed by μ-FTIR reflectance mode; however, not all particles produced interpretable spectra. Therefore, whenever adequate contact with the μ-ATR-FTIR crystal could be achieved, additional μ-ATR-FTIR analyses were performed to obtain better-defined spectra. Two representative examples of spectra acquired in both reflectance and μ -ATR-FTIR modes are shown in Figures 1 and 2.

Table 2. Characteristics of particles identified in the analyzed kidney stone samples, including the number of particles detected, particle width (µm), particles localization within the stone structure (core or intermediate layer) and particles color. Abbreviation: KS, kidney stone.

ID Sample	Particles Detected	Particles Width	Particles Location in KS	Color
1	1	10 µm	Core	dark blue
2	1	12 µm	Core	red
3	1	17 µm	Intermediate layer	white
4	1	11 µm	Intermediate layer	dark blue
5	1	17 µm	Intermediate layer	dark blue
6	1	12 µm	Intermediate layer	dark blue
7	1	10 µm	Core-intermediate layer	light blue
8	1	15 µm	not assesable	light blue

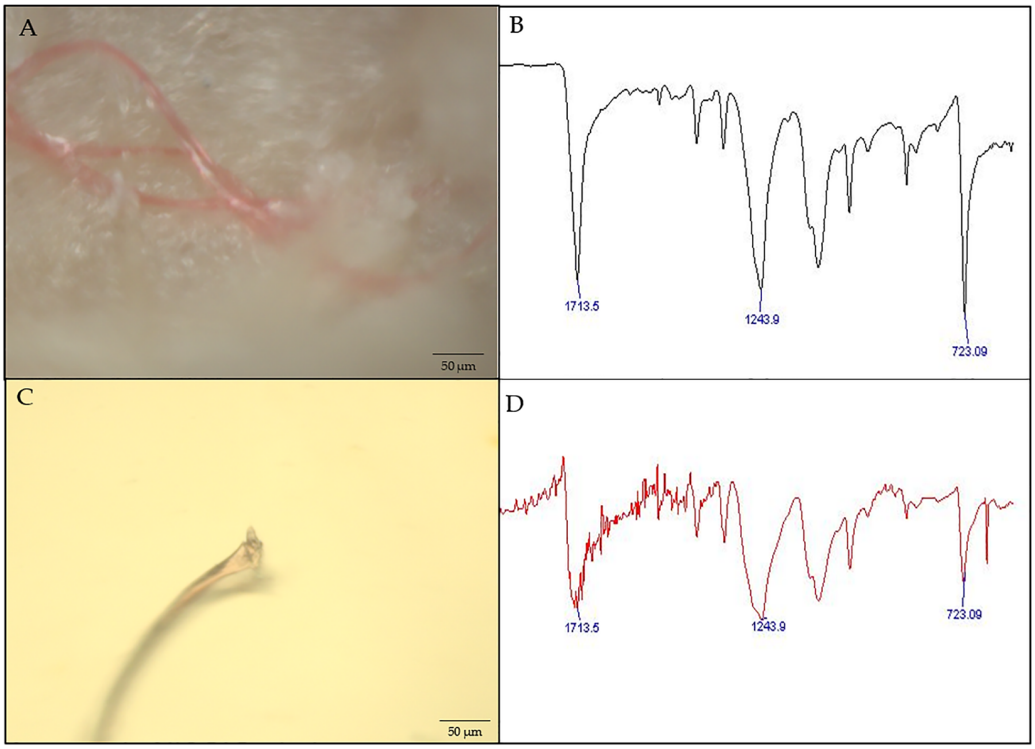


Figure 1. Representative example of optical microscopy images and spectra of selected particles isolated from kidney stone identified as PET (polyethylene terephthalate). (**A**) Microplastic particle adhered to and entrapped within the crystalline matrix of the kidney stone core. (**B**) Spectrum acquired by µ-ATR-FTIR mode, showing the detected bands at the following wavenumbers (cm^{-1}): 1713.5; 1243.9; 723.09. (**C**) Microplastic particle isolated from the kidney stone core and deposited on a gold-coated microscope slide. (**D**) Spectrum acquired by µ-FTIR-reflectance analysis, showing the detected bands at the following wavenumbers (cm^{-1}): 1713.5; 1243.9; 723.09.

µ-FTIR analysis of microplastic particles isolated from renal calculus samples indicated a heterogeneous polymer composition. Confirmed polymer assignments included polyethylene terephthalate (PET), polyethylene (PE), polypropylene (PP), and polyurethane (PU). In addition, three particles showed diagnostic µ-FTIR absorption bands compatible with polyvinyl chloride (PVC); however, these spectra were acquired in µ-FTIR-reflectance mode and were classified as organic matter by OpenSpecy. Therefore, these particles were reported as putative PVC (p-PVC) assignments. Considering both confirmed and putative polymer assignments, p-PVC compatible particles represented the most frequent finding, accounting for 37.5% (3/8) of all detected particles, followed by PET 25.0% (2/8), while PE, PP, and PU each represented 12.5% (1/8). The visual identification of PET was confirmed by the presence of its characteristic µ-FTIR bands at ~1720 cm^{-1} (ester carbonyl stretch-

ing), 1255–1245 cm^{-1} (C–O–C stretching), and ~728 cm^{-1} (aromatic C–H out-of-plane bending) [25,26]. The p-PVC assignments were based on the presence of characteristic absorption bands at 1428–1425 cm^{-1} (CH_2-Cl angular deformation), at 1337–1330 cm^{-1} (CH_2 angular deformation), 1102–1097 cm^{-1} (C-C stretching) and the band at 694–615 cm^{-1} corresponding to the stretching of C–Cl bonds [27–29]. The characteristic bands at 2915 and 2848 cm^{-1} (–CH_2 symmetric and asymmetric stretching), 1470–1462 (–CH=CH– stretching) and 720–710 cm^{-1} (–CH_2 rocking deformation) confirm the presence of polyethylene (PE) [30,31]. The polypropylene (PP) may be indicated by CH_3 deformation vibration near 1456–1455 and 1375 cm^{-1} and weaker bands in the region between 800 and 1200 cm^{-1} (808, 974 cm−1/C-C and 999, 1167 cm^{-1}/C-H) [32,33]. The polyurethane (PU) may be supposed by N-H stretch at 3326 cm^{-1}, the carbonyl stretch peaks (C=O) at 1720 and 1705 cm^{-1}, the characteristic band at 1531 cm^{-1} (N-H in-plane bending vibration) and the peak at 1222 cm^{-1} (C-O stretch) [34]. Table 3 summarizes the characteristic bands identified for the analyzed MPs and compares them with those reported in the selected literature, highlighting the correspondence between the experimental and bibliographic data.

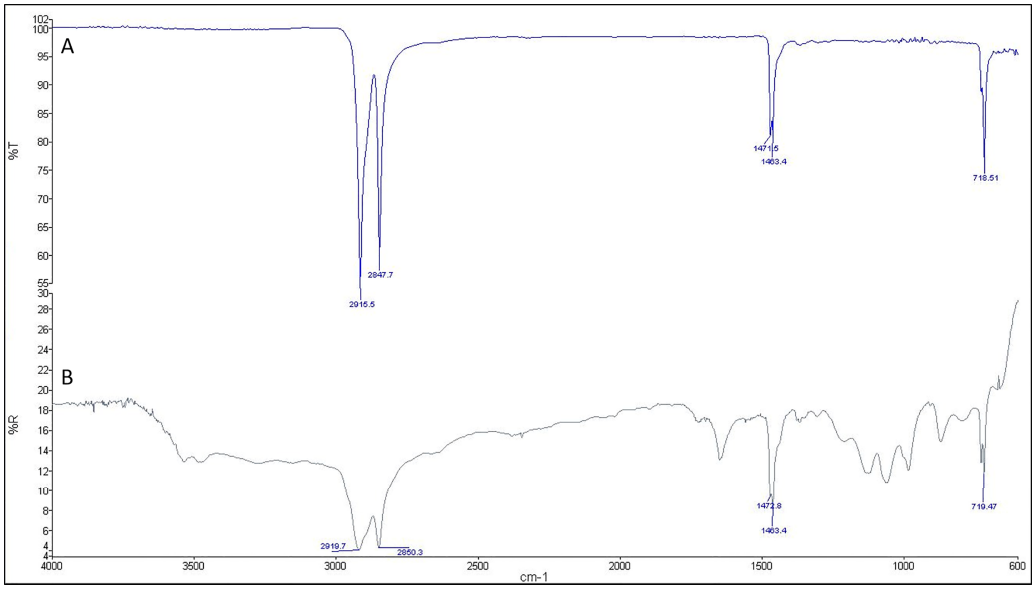


Figure 2. Comparison between a representative PE (polyethylene) particle analyzed by µ-ATR-FTIR and µ-FTIR-reflectance over the 4000–400 cm^{-1} spectral range. (**A**) Spectrum acquired by µ-ATR-FTIR analysis, showing the detected bands at the following wavenumbers (cm^{-1}): 2915.5; 2847.7; 1471.5; 1463.4; 718.51. (**B**) Spectrum of the same particle acquired by µ-FTIR-reflectance analysis showing the detected bands at the following wavenumbers (cm^{-1}): 2919.7; 2850.3; 1472.8; 1463.4; 719.47.

Following the visual inspection of the spectra and the identification of the selected diagnostic absorption bands, spectral matching against the OpenSpecy library was performed. The match value and the corresponding material class obtained for each sample are summarized in Table 4.

As expected, spectra acquired in µ-ATR-FTIR mode yielded excellent matching scores (>0.9). In contrast, spectra acquired in µ-FTIR-reflectance mode generally produced lower similarity scores, likely due to their greater spectral complexity, characterized by overlapping absorption bands.

Specifically, particles that had been assigned to p-PVC on the basis of manual spectral interpretation were classified by the library as organic matter. It is worth noting that the OpenSpecy database is primarily based on reference spectra acquired in ATR mode, which may limit its performance when applied to spectra collected in reflectance mode [24]. Considering the µ-FTIR-reflectance acquisition mode and the complex organic–mineral

matrix of renal stones, it is plausible that surface-associated organic coatings on the particles influenced the spectral response, thereby hindering unambiguous polymer identification. Therefore, the attribution of these particles to PVC was reported as putative rather than confirmed and should be interpreted with caution.

Table 3. Identification of the analyzed microplastic particles by μ-FTIR spectroscopy. Polymers identification was performed by comparing the experimentally observed absorption bands with the characteristic FTIR bands reported in the literature. PVC-compatible particles were reported as p-PVC because OpenSpecy matching did not confirm the same material class.

Sample	Polymer	Observed FTIR Bands (cm^{-1})	Diagnostic FTIR Bands (cm^{-1})	Main Vibrational Assignment	References
1	PE	2915, 2847, 1471, 1463, 718	2915–2848, 1470–1462, 720–710	CH_2 stretching, CH_2 bending, CH_2 rocking	[20,21]
2	PET	1713, 1244, 723	1721–1720, 1255–1245, 728	Ester C=O, C–O–C stretching, aromatic C–H	[15,16]
3	p-PVC	1425, 1334, 1108, 670, 616	1428–1425, 1337–1330, 1102–1097, 694–615	CH_2 deformation, C–C stretching, C–Cl stretching	[17–19]
4	PP	1455, 1375, 1168, 998, 808	1456–1455, 1375, 1167, 998–974, 808	CH_3 deformation, C–H, C–C stretching	[22,23]
5	p-PVC	1427, 1333, 1103, 670, 619	1428–1425, 1337–1330, 1102–1097, 694–615	CH_2 deformation, C–C stretching, C–Cl stretching	[17–19]
6	p-PVC	1426, 1335, 1099, 610	1428–1425, 1337–1330, 1102–1097, 694–615	CH_2 deformation, C–C stretching, C–Cl stretching	[17–19]
7	PET	1711, 1246, 730	1721–1720, 1255–1245, 728	Ester C=O, C–O–C stretching, aromatic C–H	[15,16]
8	PU	3331, 1728, 1703, 1530, 1220	3326, 1720,1705, 1531, 1222	N–H stretching, C=O stretching, N–H bending	[24]

Table 4. Material identification of the analyzed samples based on OpenSpecy spectral matching. The analytical technique used for each sample (μ-ATR-FTIR or μ-FTIR-reflectance), the OpenSpecy match value and the corresponding material class are reported.

Sample	IR Mode	Match Value	Material Class
1	Micro-ATR	0.99	poly(ethylene)
	Reflectance	0.71	poly(ethylene)
2	Micro-ATR	0.99	polyethylene terephthalate
	Reflectance	0.84	polyethylene terephthalate
3	Reflectance	0.81	organic matter
4	Micro-ATR	0.97	poly(propylene)
5	Reflectance	0.76	organic matter
6	Reflectance	0.79	organic matter
7	Reflectance	0.84	polyethylene terephthalate
8	Micro-ATR	0.93	polyurethanes

Regarding the evaluation of spectral matching performance, only one of the spectra acquired in μ-FTIR-reflectance mode showed relatively intense absorption bands consistent with PET features compared to other spectral contributions. This resulted in a library matching score above 0.84, which can be considered a good match under reflectance conditions. In addition, two representative particles were analysed using both μ-ATR-FTIR and μ-FTIR-reflectance mode. As expected, spectral matching scores obtained using μ-ATR-FRIT were consistently higher (>0.9), whereas μ-FTIR-reflectance spectra yielded lower but still

acceptable values (>0.7), reflecting the known differences in spectral quality and database compatibility between the two acquisition modes. In particular, as shown in Figure 2, the μ-FTIR-reflectance spectrum exhibits additional absorption bands compared with the μ-ATR-FTIR spectrum, which likely contributes to the lower spectral matching scores.

4. Discussion

In the present pilot biomonitoring study, polymeric particles compatible with MPs were detected in 8 of 60 human kidney stone samples by stereomicroscopic inspection followed by μ-FTIR characterization. Beyond the descriptive findings, the present study demonstrates the applicability of an analytical workflow developed within a broader One Health framework.

Although the number of positive samples was limited, the identification of polymeric particles embedded within the internal regions of renal calculi provides preliminary evidence that MPs may be incorporated into the stone structure. To our knowledge, only three previous studies have specifically investigated the occurrence of MPs in human kidney stones, making the present findings relevant for the emerging field of environmental micropollutants in urinary stone disease.

In recent years, numerous studies have demonstrated the presence of MPs in various human and animals biological matrices [35], suggesting the ability of these particles to enter the body and distribute throughout tissues. Furthermore, persistent organic pollutants have also been reported to accumulate in animal kidneys [36], supporting the kidney as a possible target of environmental contaminants.

Human exposure to micro- and nanoplastics can occur through several routes, mainly ingestion through contaminated food and drinking water, but also inhalation and, to a lesser extent, dermal contact [37].

The detection of MPs in urine supports the hypothesis that the urinary tract may represent a route of elimination for these particles, while their detection in renal tissue and kidney stones suggests that deposition or incorporation within the urinary system may also occur.

The particles identified in the present study included confirmed PET, PE, PP, and PU assignments, together with three p-PVC compatible particles. The interpretation of particles compatible with p-PVC requires caution, as these assignments were based on the presence of diagnostic absorption bands observed in the μ-FTIR-reflectance spectra, which showed a higher background noise compared with the other spectra and were therefore not confirmed by a match with OpenSpecy. In future studies, μ-ATR-FTIR spectra should be acquired to improve spectral quality and interpretation and to further reduce the possibility of obtaining spectra that are difficult to interpret.

Nevertheless, PVC compatible particles represented the most frequent putative polymer assignment in the present series. This finding is partially consistent with the results reported by Zeng et al. [17], who identified PE and PVC among the most prevalent microplastic polymers in human kidney stones.

The authors further demonstrated that exposure to MPs may be associated with mitochondrial oxidative stress, metabolic alterations, and inflammatory processes in renal cells. Furthermore, PVC has also been identified in human urine, suggesting that this polymer may reach the urinary tract [16]. In contrast, the PU particle identified in our study should be interpreted with caution, because it was detected in a disintegrated specimen in which the original localization within the stone matrix could not be reliably assessed. Therefore, unlike the other polymers detected within intact stone structures, the PU particle cannot be considered with certainty as plastic material originally present within the analyzed kidney stone.

Experimental evidence indicates that damage to renal epithelial cells can increase interaction with calcium oxalate crystals. MPs can affect renal tubular cells through a combination of oxidative imbalance, mitochondrial dysfunction, metabolic alterations, and inflammation, compromising epithelial homeostasis and making the tubular surface more susceptible to interaction with urinary crystals [38,39].

Therefore, epithelial damage could represent a potential link between microplastic nephrotoxicity and stone formation.

It is still unclear whether MPs simply incorporate into preexisting stones or directly influence their formation. An active role would require demonstrating that MPs modify crystal behavior or increase stone formation, while their presence without such modifications would be more consistent with passive incorporation. Recent findings related to polystyrene nanoplastics support the possibility of an active contribution [19]. However, these findings are primarily derived from experimental models. Further studies are therefore needed to determine whether MPs are passive components of kidney stones or actively contribute to the formation and retention of crystals.

However, some hypotheses can be considered. MPs have irregular surfaces and may adsorb proteins or other organic molecules. These characteristics could theoretically favor interactions with urinary crystals and with the organic matrix of the stone. In this context, MPs may behave as non-crystalline particles incorporated into a growing calculus, potentially facilitating local crystal adhesion or aggregation. This interpretation is consistent with current concepts of stone formation, in which supersaturation alone is not sufficient and local surfaces, organic matrix components, and crystal retention play an important role in lithogenesis.

The relatively low number of detected microplastic particles compared with previous studies may be explained by the conservative analytical strategy adopted. Only particles visually identified under the stereomicroscope and embedded within the core or middle region of the kidney stones were analysed, whereas no complete chemical digestion of the mineral matrix was performed. This approach was intentionally chosen to minimize additional sample handling and thereby reduce the risk of pre-analytical contamination, which has been widely recognized as a major challenge in microplastic analysis of biological matrices. Although this strategy likely underestimated the total microplastic burden by excluding particles not directly visible or still embedded within the matrix, it increased confidence that the analysed particles originated from the kidney stones rather than from laboratory contamination.

In addition, procedural blank controls were performed for each analytical session to monitor potential airborne or procedural contamination during sample handling and microplastic identification. All procedures were conducted under a laminar flow hood to minimize environmental contamination. Additionally, the water used for washing renal calculi to remove loosely attached particles was pre-filtered using 0.45 μm filters. During each analysis session, a clean glass slide was placed under the stereomicroscope within the laminar flow hood and subsequently examined to assess potential airborne particle deposition during the identification process. All blank controls consistently showed no detectable particulate contamination. These results indicate that the observed MPs are unlikely to be attributable to laboratory or environmental contamination introduced during sample processing. Based on these quality assurance measures, the PET and PE particles are considered strongly associated with the stone matrix, as they were observed embedded within the crystalline core of the calculi, suggesting incorporation into the stone structure rather than surface contamination. In contrast, the PU particle was identified in one specimen that arrived at the laboratory completely disintegrated into loose crystalline material. Unlike intact stones, this sample no longer preserved its original architecture,

making it impossible to determine whether the detected PU particle had been originally embedded within the calculus or introduced during clinical handling. PU has been found in several human samples [40] and recently in urinary stones [18], but it must also be considered that it is commonly present in medical devices and surgical materials [41] so an exogenous origin cannot be ruled out. This observation further underscores the need for rigorous contamination control at all stages of sample collection and processing, as recently discussed in studies addressing contamination risks in micro- and nanoplastic research [42,43]. Accordingly, while the analytical workflow demonstrates a high level of contamination control, the possibility that certain particles may originate from clinical interventions rather than endogenous incorporation should be considered.

This may be addressed in future studies by monitoring all stages of the process, from the clinical and surgical setting through to sample delivery to the laboratory.

The ability to monitor the entire workflow, from the clinical department where the kidney stones are collected to their delivery to the laboratory, would provide valuable clinical information for interpreting environmental exposure, which is currently lacking in this preliminary study.

Future studies integrating longitudinal clinical data and detailed exposure histories are needed to validate the potential of kidney stones as a matrix for long-term exposure biomonitoring.

This study has several limitations. First, only particles visible under a stereomicroscope were investigated, and their identification was performed exclusively using μ-FTIR spectroscopic techniques. This methodological approach may have underestimated the actual microplastic burden, particularly for very small MPs and nanoplastics.

In addition, although contamination control procedures were adopted, pre-analytical contamination during sample collection or handling cannot be completely excluded.

Future studies could use renal cell organoids to investigate the potential interaction between MPs and kidney stone formation. Different microplastic polymers, including those most frequently reported in the literature and those identified in our study, could be tested alone and together with calcium oxalate or calcium phosphate crystals, the main mineral components of kidney stones. Changes in crystal characteristics and epithelial crystal interactions could be evaluated together with oxidative stress and inflammatory markers. Comparisons between controls, crystals alone, MPs alone, and combined exposure would help determine whether MPs enhance crystal-induced injury or influence processes involved in crystal formation and retention.

In addition, future studies should include larger cohorts, systematic analysis of both kidney stones and paired urine samples, and detailed information on dietary habits, environmental exposure, and clinical-metabolic risk factors for urolithiasis. Advanced analytical techniques, such as Pyrolysis–Gas Chromatography–Mass Spectrometry (Py-GC-MS), may also help to improve polymer identification and quantify smaller particles, including nanoplastics. These approaches will be necessary to clarify whether MPs are incidental inclusions in kidney stones or may contribute to stone formation and progression.

5. Conclusions

This pilot study demonstrates the successful application of a μ-FTIR analytical workflow for detecting and characterizing MPs embedded within human kidney stones. Beyond documenting the occurrence of PET, PE, PP, PU and putative PVC particles in a previously unexplored pathological biomineral, these findings support the translation of an integrated One Health biomonitoring platform across diverse biological matrices. Kidney stones may represent a valuable matrix for investigating long-term exposure to environmental MPs and complement analyses performed in urine, organoid models and other biological specimens.

Further studies integrating molecular, multi-omics and clinical data are warranted to clarify whether MPs represent passive inclusions or actively contribute to nephrolithiasis.

Author Contributions: Conceptualization, A.P., A.U. and J.G.; Methodology, A.P. and J.G.; Validation, A.P., J.G. and M.C.; Formal Analysis, A.P., L.S. and M.C.; Investigation, A.P., J.G., L.S. and M.C.; Resources, S.P. and L.S.; Data Curation, A.P., M.C. and L.S.; Writing—Original Draft, A.P. and J.G.; Writing—Review and Editing, A.P., J.G., M.C., S.P., L.S., P.R. and A.U.; Visualization, A.P., S.P. and L.S.; Supervision, A.P. and J.G.; Project Administration, J.G., P.R. and A.U.; Funding Acquisition, P.R. and A.U. All authors have read and agreed to the published version of the manuscript.

Funding: This research was also partially funded by the European Union—Next Generation EU—PNRR M6C2 (National Recovery and Resilience Plan); Investment 2.1 Enhancement and strengthening of biomedical research in the National Health Service, grant number PNRR-POC-2022-12376208–CUP: C53C22001220007 and Minister of University and Research PRIN: PROGETTI DI RICERCA DI RILEVANTE INTERESSE NAZIONALE—Bando 2022—PROT # 2022EWTKNK.

Institutional Review Board Statement: The study adhered to the principles outlined in the 1964 Declaration of Helsinki and its subsequent revisions. The study was approved by the Comitato Etico Territoriale Lazio Area 3 at the Fondazione Policlinico Agostino Gemelli IRCCS (protocol ID 5490-approval date: 9 February 2023).

Informed Consent Statement: Only residual samples from routine laboratory diagnostic procedures were used. For this reason, informed consent for participation was not required. These residual samples were used exclusively to develop and optimize a procedure for the identification and characterization of microplastics in kidney stones.

Data Availability Statement: The data presented in this study are available on request from the corresponding author.

Acknowledgments: This work represents one of the translational activities developed within the PNRR-funded project "Integrated One Health-OMICS to identify the impacts of microplastics (I-OHM)", aimed at developing standardized analytical platforms for the detection and biological characterization of microplastics across environmental and human biological matrices.

Conflicts of Interest: The authors declare no conflicts of interest.

Abbreviations

The following abbreviations are used in this manuscript:

MPs	Microplastics
μ-FTIR	Fourier-transform infrared microspectroscopy
μ-ATR-FTIR	micro-attenuated total reflectance Fourier-transform infrared spectroscopy
μ-FTIR reflectance	Fourier-transform infrared (FTIR) microspectroscopy in reflectance mode
ATR	attenuated total reflectance
PET	polyethylene terephthalate
PE	polyethylene
PP	polypropylene
PU	polyurethane
PVC	polyvinyl chloride
p-PVC	putative PVC
COM	calcium oxalate monohydrate
COD	calcium oxalate dihydrate
CA	carbonate apatite
PAM	magnesium ammonium phosphate
AU0	anhydrous uric acid
AU2	dihydrate uric acid

AmUr	ammonium urate
PR	proteins

References

1. Angelopoulos, P.; Neofytoy, P.; Katsimperis, S.; Triantafylloy, P.; Manolitsis, I.; Lardas, M.; Markopoulos, T.; Varkarakis, I.; Tzelves, L.; Skolarikos, A. Metabolic evaluation of urolithiasis: A narrative review. *Die Urol.* **2025**, *64*, 680–685. [CrossRef] [PubMed]
2. GBD 2021 Urolithiasis Collaborators. The global, regional, and national burden of urolithiasis in 204 countries and territories, 2000–2021: A systematic analysis for the Global Burden of Disease Study 2021. *eClinicalMedicine* **2024**, *78*, 102924. [CrossRef] [PubMed]
3. Skolarikos, A.; Geraghty, R.; Somani, B.; Tailly, T.; Jung, H.; Neisius, A.; Petřík, A.; Kamphuis, G.M.; Davis, N.; Bezuidenhout, C.; et al. European Association of Urology Guidelines on the Diagnosis and Treatment of Urolithiasis. *Eur. Urol.* **2025**, *88*, 64–75. [CrossRef] [PubMed]
4. Dong, C.; Yang, Y.; Cheng, B.; Yang, S.; Wang, Y. Environmental determinants in the development of kidney stone. *Urolithiasis* **2025**, *53*, 43. [CrossRef] [PubMed]
5. Sun, Y.; Zhou, Q.; Zheng, J. Nephrotoxic metals of cadmium, lead, mercury and arsenic and the odds of kidney stones in adults: An exposure-response analysis of NHANES 2007–2016. *Environ. Int.* **2019**, *132*, 105115. [CrossRef] [PubMed]
6. Pięta, J.; Szyszka, M.; Lipiński, P.; Skrzypczyk, P. Urolithiasis in Children-Clinical Picture, Pathogenesis, and Diagnostic Approach. *Biomolecules* **2026**, *16*, 119. [CrossRef] [PubMed]
7. Tamborino, F.; Cicchetti, R.; Mascitti, M.; Litterio, G.; Orsini, A.; Ferretti, S.; Basconi, M.; De Palma, A.; Ferro, M.; Marchioni, M.; et al. Pathophysiology and Main Molecular Mechanisms of Urinary Stone Formation and Recurrence. *Int. J. Mol. Sci.* **2024**, *25*, 3075. [CrossRef] [PubMed]
8. Evan, A.P.; Worcester, E.M.; Coe, F.L.; Williams, J., Jr.; Lingeman, J.E. Mechanisms of human kidney stone formation. *Urolithiasis* **2015**, *43*, 19–32. [CrossRef] [PubMed]
9. Suttapitugsakul, S.; Peerapen, P.; Thongboonkerd, V. Promoting Effects of Urinary Proteins from Stone Formers and Influence of Their Physicochemical Properties on Calcium Oxalate Kidney Stone Formation. *Comput. Struct. Biotechnol. J.* **2026**, *35*, 0094. [CrossRef] [PubMed]
10. Prata, J.C.; da Costa, J.P.; Lopes, I.; Andrady, A.L.; Duarte, A.C.; Rocha-Santos, T. A One Health perspective of the impacts of microplastics on animal, human and environmental health. *Sci. Total Environ.* **2021**, *777*, 146094. [CrossRef] [PubMed]
11. Cole, M.; Lindeque, P.; Halsband, C.; Galloway, T.S. Microplastics as contaminants in the marine environment: A review. *Mar. Pollut. Bull.* **2011**, *62*, 2588–2597. [CrossRef] [PubMed]
12. Zuri, G.; Karanasiou, A.; Lacorte, S. Human biomonitoring of microplastics and health implications: A review. *Environ. Res.* **2023**, *237*, 116966. [CrossRef] [PubMed]
13. Leonard, S.V.L.; Liddle, C.R.; Atherall, C.A.; Chapman, E.; Watkins, M.; Calaminus, S.D.J.; Rotchell, J.M. Microplastics in human blood: Polymer types, concentrations and characterisation using μFTIR. *Environ. Int.* **2024**, *188*, 108751. [CrossRef] [PubMed]
14. Li, Y.; Chen, L.; Zhou, N.; Chen, Y.; Ling, Z.; Xiang, P. Microplastics in the human body: A comprehensive review of exposure, distribution, migration mechanisms, and toxicity. *Sci. Total Environ.* **2024**, *946*, 174215. [CrossRef] [PubMed]
15. Massardo, S.; Verzola, D.; Alberti, S.; Caboni, C.; Santostefano, M.; Eugenio Verrina, E.; Angeletti, A.; Lugani, F.; Ghiggeri, G.M.; Bruschi, M.; et al. MicroRaman spectroscopy detects the presence of microplastics in human urine and kidney tissue. *Environ. Int.* **2024**, *184*, 108444. [CrossRef] [PubMed]
16. Pironti, C.; Notarstefano, V.; Ricciardi, M.; Motta, O.; Giorgini, E.; Montano, L. First Evidence of Microplastics in Human Urine, a Preliminary Study of Intake in the Human Body. *Toxics* **2023**, *11*, 40. [CrossRef] [PubMed]
17. Zeng, Q.; Tang, J.; Zhan, L.; Liang, R.; Yang, C.; Cai, R.; Luo, J.; Xu, J.; Liu, T.; Wei, H.; et al. Multimodal detection of microplastics in human kidney stones and multi-omics exploration of renal cell metaflammation. *J. Hazard. Mater.* **2026**, *512*, 142443. [CrossRef] [PubMed]
18. Carrier, K.; Garcia, M.; Campen, M.J.; Patil, S.; El Hayek, E.; Kotulski, J.; Davis, M. Microplastics in Urinary Calculi: Evidence from Human Urinary Stones. *J. Urol.* **2026**. [CrossRef] [PubMed]
19. Su, X.; Yang, Y.; Xiang, H.; Dong, C.; Shi, M.; Wang, Y.; Zhou, Q.; Song, Q.; He, Z.; Jiang, Q.; et al. Supplemental exposure to polystyrene nanoplastics synergistically amplifies calcium oxalate crystal-induced injury to renal tubular epithelium, accelerating the formation of calcium oxalate kidney stones. *Part. Fibre Toxicol.* **2026**, *23*, 8. [CrossRef] [PubMed]
20. Dawson, A.L.; Bose, U.; Ni, D.; Nelis, J.L.D. Unravelling protein corona formation on pristine and leached microplastics. *Microplastics Nanoplastics* **2024**, *4*, 9. [CrossRef]
21. Lujic, T.; Mutic, T.; Simovic, A.; Vasovic, T.; Ivanovic, S.; Krstic Ristivojevic, M.; Jovanovic, V.; Cirkovic Velickovic, T. Protein Corona Stability and Removal from PET Microplastics: Analytical and Spectroscopic Evaluation in Simulated Intestinal Conditions. *Foods* **2025**, *14*, 3454. [CrossRef] [PubMed]

22. Primiano, A.; Persichilli, S.; Ferraro, P.M.; Minucci, A.; Gambaro, G.; Urbani, A.; Gervasoni, J. A combination of infrared spectroscopy and morphological analysis allows successfully identifying rare crystals and atypical urinary stones. *Ann. Ist. Super. Sanità* **2019**, *55*, 205–208. [CrossRef] [PubMed]
23. Cowger, W.; Steinmetz, Z.; Gray, A.; Munno, K.; Lynch, J.; Hapich, H.; Primpke, S.; De Frond, H.; Rochman, C.; Herodotou, O. Microplastic Spectral Classification Needs an Open Source Community: Open Specy to the Rescue! *Anal. Chem.* **2021**, *93*, 7543–7548. [CrossRef] [PubMed]
24. Cowger, W.; Roscher, L.; Jebens, H.; Chamas, A.; Maurer, B.D.; Gehrke, L.; Gerdts, G.; Primpke, S. Generation of macro- and microplastic databases by high-throughput FTIR analysis with microplate readers. *Anal. Bioanal. Chem.* **2024**, *416*, 1311–1320. [CrossRef] [PubMed]
25. Smith, B.C. Infrared Spectroscopy of Polymers, VIII: Polyesters and the Rule of Three. *Spectroscopy* **2022**, *37*, 25–28. [CrossRef]
26. Chen, Z.; Hay, J.N.; Jenkins, M.J. FTIR spectroscopic analysis of poly(ethylene terephthalate) on crystallization. *Eur. Polym. J.* **2012**, *48*, 1586–1610. [CrossRef]
27. Park, E.J.; Park, B.C.; Kim, Y.J.; Canlier, A.; Hwang, T.S. Elimination and Substitution Compete During Amination of Poly(vinyl chloride) with Ehtylenediamine: XPS Analysis and Approach of Active Site Index. *Macromol. Res.* **2018**, *26*, 913–923. [CrossRef]
28. Coltro, L.; Pitta, J.B.; Madaleno, E. Performance evaluation of new plasticizers for stretch PVC films. *Polym. Test.* **2013**, *32*, 272–278. [CrossRef]
29. Lee, C.S.; Adam, M.; Robinson, J.P.; Binner, E.R. Highly efficient and rapid dechlorination of polyvinyl chloride via microwave pyrolysis. *Philos. Trans. A Math. Phys. Eng. Sci.* **2025**, *383*, 20240064. [CrossRef] [PubMed]
30. Campanale, C.; Savino, I.; Massarelli, C.; Uricchio, V.F. Fourier Transform Infrared Spectroscopy to Assess the Degree of Alteration of Artificially Aged and Environmentally Weathered Microplastics. *Polymers* **2023**, *15*, 911. [CrossRef] [PubMed]
31. Dobrzyńska-Mizera, M.; Knitter, M.; Piss, M.; Del Barone, C.; Mallardo, S.; Santagata, G.; Di Lorenzo, M.L. Thermal and Morphological Analysis of Linear Low-Density Polyethylene Composites Containing d-limonene/β-cyclodextrin for Active Food Packaging. *Molecules* **2023**, *28*, 1220. [CrossRef] [PubMed]
32. Ramos, V.S.; Dias, M.L. Refined Analysis of Microplastics: Integrating Infrared and Raman Spectroscopy. *An. DA Acad. Bras. DE Ciênc.* **2025**, *97*, e20241313. [CrossRef] [PubMed]
33. Böke, J.S.; Popp, J.; Krafft, C. Optical photothermal infrared spectroscopy with simultaneously acquired Raman spectroscopy for two-dimensional microplastic identification. *Sci. Rep.* **2022**, *12*, 18785. [CrossRef] [PubMed]
34. Smith, B.C. Infrared Spectroscopy of Polymers XIII: Polyurethanes. *Spectroscopy* **2023**, *38*, 14–16. [CrossRef]
35. Prata, J.C.; Silva, A.L.P.; da Costa, J.P.; Dias-Pereira, P.; Carvalho, A.; Fernandes, A.J.S.; da Costa, F.M.; Duarte, A.C.; Rocha-Santos, T. Microplastics in Internal Tissues of Companion Animals from Urban Environments. *Animals* **2022**, *12*, 1979. [CrossRef] [PubMed]
36. Nomiyama, K.; Sato, R.; Sato, F.; Eguchi, A. Accumulation of persistent organic pollutants in the kidneys of pet cats (Felis silvestris catus) and the potential implications for their health. *Sci. Total Environ.* **2024**, *933*, 173212. [CrossRef] [PubMed]
37. Barceló, D.; Picó, Y.; Alfarhan, A.H. Microplastics: Detection in human samples, cell line studies, and health impacts. *Environ. Toxicol. Pharmacol.* **2023**, *101*, 104204. [CrossRef] [PubMed]
38. Kehinde, S.A.; Olajide, A.T.; Ogunsanya, S.T.; Fatokun, T.P.; Olulana, D.I.; Olabiyi, F.A.; Faokunla, O.; Tham, C.L.; Chusri, S. Polyethylene microplastics disrupt renal function, mitochondrial bioenergetics, redox homeostasis, and histoarchitecture in Wistar rats. *Sci. Rep.* **2025**, *15*, 41120. [CrossRef] [PubMed]
39. Han, J.; Guo, D.; Sun, X.Y.; Wang, J.M.; Ouyang, J.M.; Gui, B.S. Comparison of the adhesion and endocytosis of calcium oxalate dihydrate to HK-2 cells before and after repair by Astragalus polysaccharide. *Sci. Technol. Adv. Mater.* **2019**, *20*, 1164–1177. [CrossRef] [PubMed]
40. Vdovchenko, A.; Resmini, M. Mapping Microplastics in Humans: Analysis of Polymer Types, and Shapes in Food and Drinking Water-A Systematic Review. *Int. J. Mol. Sci.* **2024**, *25*, 7074. [CrossRef] [PubMed]
41. Braun, T.; Ehrlich, L.; Henrich, W.; Koeppel, S.; Lomako, I.; Schwabl, P.; Liebmann, B. Detection of Microplastic in Human Placenta and Meconium in a Clinical Setting. *Pharmaceutics* **2021**, *13*, 921. [CrossRef] [PubMed]
42. Baroni, A.; Romano, E.; Pulone, S.; Moulton, C.; Tasciotti, E. Plastic-on-Plastic: Underestimated Contamination Risks in Micro- and Nanoplastic Research. *Earth Environ. Sustain.* **2026**, *2*, 183–199. [CrossRef]
43. Lao, W.; Sauers, S.; Wong, C.S. Characterization and potential influence of laboratory airborne particle fallout on microplastics analysis. *J. Hazard. Mater.* **2025**, *499*, 140309. [CrossRef] [PubMed]

Disclaimer/Publisher's Note: The statements, opinions and data contained in all publications are solely those of the individual author(s) and contributor(s) and not of MDPI and/or the editor(s). MDPI and/or the editor(s) disclaim responsibility for any injury to people or property resulting from any ideas, methods, instructions or products referred to in the content.